A Heterogeneously Integrated III-V Membrane on Silicon-On-Insulator for All-Optical Signal Processing Applications

M. Tassaert,[1] G. Roelkens,[1] H. J. S. Dorren,[2] D. Van Thourhout,[1] and O. Raz[2]

[1] INTEC, Ghent University—imec, Sint-Pietersnieuwstraat 41, 9000 Ghent, Belgium
[2] Eindhoven University of Technology, Den Dolech 2, 5600MB, Eindhoven, The Netherlands

A new device in the hybrid III-V on Silicon-On-Insulator (SOI) toolbox is proposed for all-optical signal processing applications. The membrane InP switch (MIPS) consists of a bonded III-V membrane waveguide of only 100 nm thick which is coupled to the underlying SOI circuit. Because of the high index contrast between the III-V membrane and the surrounding cladding, a high confinement of light is achieved in the active region of the device, leading to compact devices that can be optically pumped with a strong light-matter interaction. Operation as an optical amplifier, all-optical switch and passive regenerator is demonstrated.

Introduction

Silicon-On-Insulator (SOI) is an excellent platform for the realization of passive optical functions. The high index contrast waveguides that can be achieved show low loss and allow for very tight bends, reducing the footprint of photonic integrated circuits. Furthermore, the fabrication of SOI photonic integrated circuits is CMOS compatible, and therefore allows for integration of both electronics and photonics on a single die. However, most applications also require active optical functions, such as lasers and detectors. Due to silicon's indirect band gap, creating active devices on SOI remains a challenge. Several approaches exist to address this [1], however currently the most successful demonstrations are based on heterogeneous integration of an active III–V layer stack on top of the SOI waveguide circuit [2-3]. This can be achieved either by direct die-to-wafer bonding or adhesive die-to-wafer bonding, using DVS-BCB as an intermediate adhesive between the SOI circuit and III–V layers. In these approaches however, one typically uses a thick III-V waveguide with a thickness of more than 500 nm, to ensure efficient current injection in the device. This limits the maximal confinement of the optical mode in the active layers however, reducing the strength of the light-matter interaction, leading to longer devices with higher power consumption. If optical excitation were used instead of electrical pumping however, the device thickness could be dramatically reduced, as current injection and ohmic contacts would no longer be required. As a result, one can leverage the high index contrast between the high index III-V and surrounding low index DVS-BCB/SiO_2 cladding layers to achieve a much higher confinement in the active layers.

In this paper, we present the membrane InP switch (MIPS), which consists of a 100 nm thick membrane ridge waveguide coupled to an underlying silicon circuit. Due to the high confinement of light, a strong light-matter interaction is achieved, which limits the device footprint and operating power. Optical amplification, regeneration action and switching of packets are demonstrated.

Device layout

The device structure of the MIPS is schematically shown in Fig. 1(a). It consists of two silicon access waveguides which are coupled to a III-V membrane waveguide by two inverted taper couplers. These couplers are designed to support an adiabatic transition between the fundamental TE mode in the silicon wire and III-V membrane for bonding layer thicknesses of <150 nm and lithographic alignment error of <250 nm. They consist of a linearly tapered 220 nm thick silicon wire of 18 µm long, starting from a width of 700 nm and tapering down to a width of 100 nm, while the III-V membrane on top tapers from 1 µm to 1.5 µm. The III-V membrane consists of 3 InGaAsP quantum wells of 8 nm thick, separated by InP barriers of 10 nm thick and sandwiched between two InP cladding layers of 25 nm thick. This quantum well stack has a band gap wavelength of ≈ 1.58 µm. The III-V membrane waveguide is a ridge waveguide formed by shallow dry etching of the bonded III-V stack to a remaining ridge thickness of ≈ 25 nm. In Fig. 1(b), the fundamental TE-mode is shown for the resulting waveguide. The high intensity in the active region can be clearly seen and a confinement of 17% is reached. Furthermore, the remaining InP ridge on the sides reduces the thermal resistance of the device considerably, allowing for better performance [4].

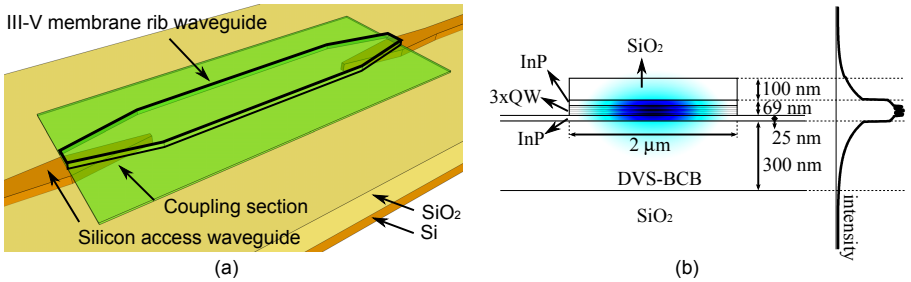

Fig. 1 (a) Schematic view of the MIPS [5]. (b) Mode profile in the membrane rib waveguide with plot of the intensity in the center of the waveguide [5].

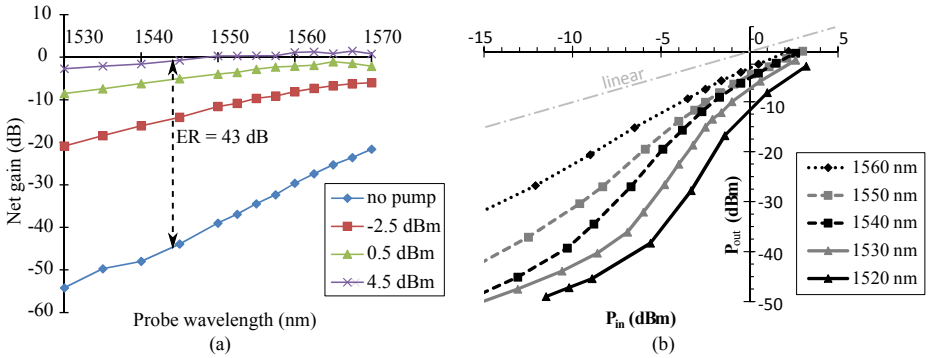

Fig. 2 (a) Probe transmission as a function of wavelength for different on-chip pump powers [5]. (b) Transmission through the MIPS as a function of on-chip input power for different wavelengths [6].

Amplification

A first application of the MIPS is on-chip amplification of optical signals. To determine the net gain that can be achieved, a pump-probe experiment was performed [5], in which a strong pump signal at a wavelength of 1505 nm is combined with a probe signal with an input power of only -19 dBm. By comparing the probe transmission to a

reference measurement, the net gain can be extracted. The results for a 150 µm long device are shown in Fig. 2(a). As can be seen, the device absorption can be bleached using low pump powers and an extinction of 30 to 40 dB can be achieved between the pumped state and the unpumped state for wavelengths in the C-band. However, the gain is limited: due to a combination of thermal effects and reduced pump absorption, the achieved gain is limited to 2 dB. However, if one could further reduce the thermal resistivity of the device, higher CW gains should be possible [4].

Regeneration

In Fig. 2(b) the transmission of a signal through the MIPS as a function of input power is shown. One can identify three regimes in these curves. For low input signal power, the transmission curve shows a linear relation. This is the case because the number of generated carriers by signal absorption is negligible and therefore the device absorption is not bleached and remains at a high value. When power increases however, the number of generated carriers increases as well and starts decreasing the device absorption. This leads a strong non-linear behaviour in the transmission curve *($\partial P_{out}/\partial P_{in} > 1$)*. For a high input power on the other hand, the transmission curve again shows a linear relation. In this case, the number of generated carriers is high enough to completely bleach the device absorption. In the regime of non-linear transmission, the MIPS could operate as a regenerator, as a slight change in input power can lead to a much higher change in output power. To demonstrate this, a bit error rate (BER) measurement was performed [6], where a signal with only 2 dB extinction was transmitted through the device. This signal was imprinted with a pseudorandom binary sequence (PRBS) of $2^{31} - 1$ bits using non return to zero on-off keying (NRZ-OOK) at a speed of 1 Gb/s. The results are shown in Fig. 3(a) and a corresponding eye pattern is given in Fig. 3(b). Compared to a back-to-back (B2B) measurement, a receiver sensitivity improvement of 4.5 dB is achieved at a wavelength of 1530 nm.

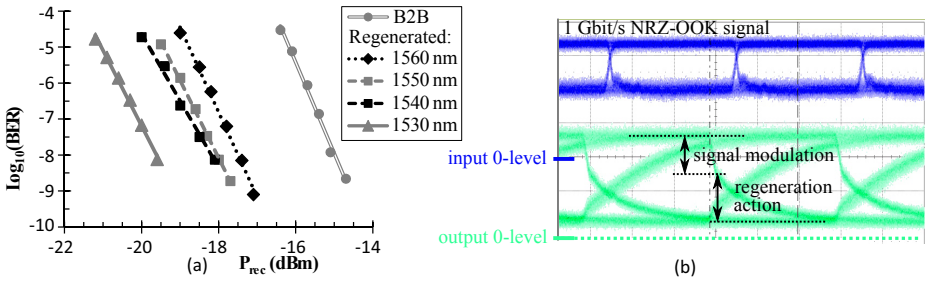

Fig. 3 (a) Results of BER measurement showing a clear improvement due to regeneration [6]. (b) Eye diagram showing the input signal before and after transmission through the MIPS [6].

Packet switching

The MIPS can also be used as a component to obtain packet switching. As can be seen in Fig. 2(a), a small amount of pump power can yield a huge extinction in the probe signal. By placing the MIPS within a broadcast-and-select architecture [5] (see Fig. 4(a)), a signal with wavelength in the C-band can be routed from one input port to several output ports, depending on the wavelength of the label. In this architecture, first the label is separated from the signal, using a Mach-Zehnder interferometer (MZI).

Afterwards, the label is processed by an arrayed waveguide grating (AWG). At the same time, the signal is broadcast by a splitter tree and combined with the AWG outputs and sent to the output branches. There, depending on the presence of a label, which acts as a pump for the MIPS, the MIPS will transmit or block the signal. To demonstrate the feasibility of such a switch, a proof-of-concept measurement was performed [5] in which a series of packets encoded using a PRBS of $2^{31} - 1$ bits with NRZ-OOK is sent through a single MIPS at 20 Gb/s at a wavelength of 1542.5 nm. A 1505 nm pump bleaches the absorption of the MIPS during the packets, but is off in between two packets. In figure 4(b) the BER is plotted comparing the back-to-back measurement to the measurement using the MIPS. As can be seen, there is no switch-related power penalty, proving that the MIPS does not interfere with the signal when switched on.

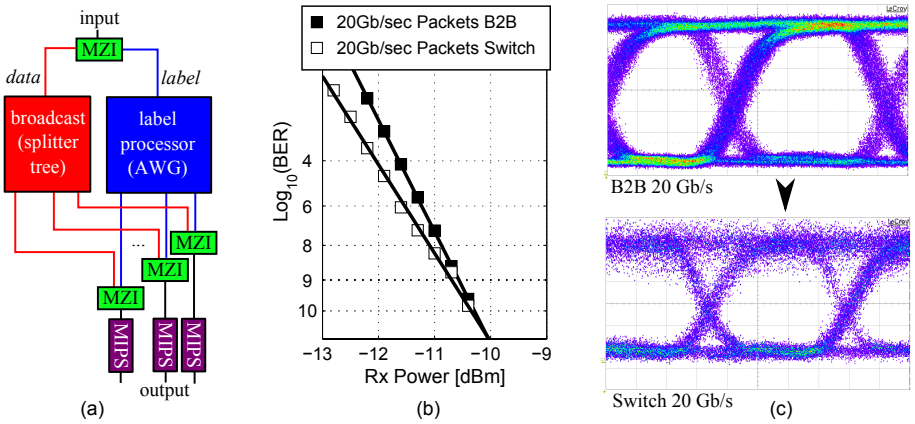

Fig. 4 (a) Proposed packet switch architecture. (b) Results of BER measurement [5]. (c) Eye diagrams showing the back-to-back (top) and transmitted through switch signals (bottom). The additional noise in the transmitted signal is due to the necessity of amplifying the transmitted signal with an EDFA [5].

Conclusion

In this paper we have presented the membrane InP switch (MIPS) as a new device in the hybrid III-V/SOI toolbox. Due to the strong light-matter interaction, this device is ideal to perform signal processing applications such as regeneration and switching. In future work, the device will be improved by reducing carrier lifetime to reach higher speeds and by reducing the device width to lower the power consumption.

References

[1] B. Jalali, and S. Fathpour, "Silicon photonics," J. Lightwave Technol. **24**(12), 4600-4615 (2006).

[2] S.R. Jain, M.N. Sysak, G. Kurczveil, and J.E. Bowers, "Integrated hybrid silicon DFB laser-EAM array using quantum well intermixing," Opt. Express **19**, 13692-13699 (2011).

[3] G. Roelkens, L. Liu, D. Liang, R. Jones, A. Fang, B. Koch, and J. Bowers, "III-V/silicon photonics for on-chip and inter-chip optical interconnects," Laser Photon. Rev. **4**(6), 751-779 (2010).

[4] M. Tassaert, S. Keyvaninia, D. Van Thourhout, W.M.J. Green, Y. Vlasov, G. Roelkens, "An optically pumped nanophotonic InP/InGaAlAs optical amplifier integrated on a SOI waveguide circuit," Opt. and Quantum Electron. (invited), **44**(12), 513-519 (2012)

[5] M. Tassaert, G. Roelkens, H. Dorren, D. Van Thourhout, and O. Raz, "Bias-free, low power and optically driven membrane InP switch on SOI for remotely configurable photonic packet switches," Opt. Express **19**, B817-B824 (2011).

[6] M. Tassaert, H. Dorren, G. Roelkens, and O. Raz, "Passive InP regenerator integrated on SOI for the support of broadband silicon modulators," Opt. Express **20**, 11383-11388 (2012).